ORIGINAL PAPER

Quantification accuracy in photon-counting detector CT for coronary artery calcium score: a pilot study

Mengzhen Wang[1] · Xu Zhang[1] · Jiqang Li[1] · Haipeng Dong[1] · Zhihan Xu[2] · Fuhua Yan[1] · Wenjie Yang[1]

Abstract

To validate the accuracy of coronary artery calcium score (CACS) using photon-counting detector (PCD) CT under various scanning settings and explore the optimized scanning settings considering both the accuracy and the radiation dose. A CACS phantom containing six hollow cylindrical hydroxyapatite calcifications of two sizes with three densities and 12 patients underwent CACS scans. For PCD-CT, two scanning modes (sequence and flash [high-pitch spiral mode]) and five tube voltages (90kV, 120kV, 140kV, Sn100kV, and Sn140kV) at different image quality (IQ) levels were set for phantom, and patients were scanned with 120kV at IQ19 using flash mode. All acquisitions from PCD-CT were reconstructed at 70keV. Acquisitions in sequence mode at 120kV on an energy-integrating detector CT (EID-CT) was used as the reference. Agatston, mass, and volume scores were calculated. The CACS from PCD-CT exhibited excellent agreements with the reference (all intraclass correlation coefficient [ICC] > 0.99). The root mean square error (RMSE) between the Agatston score acquired from PCD-CT and the reference (5.4–11.5) was small. A radiation dose reduction (16–75%) from PCD-CT compared with the reference was obtained in all protocols using flash mode, albeit with IQ20 only at sequence mode (22–44%). For the patients, ICC (all ICC > 0.98) and Bland–Altman analysis of CACS all showed high agreements between PCD-CT and the reference, without reclassifying CACS categories(P = 0.317). PCD-CT yields repeatable and accurate CACS across diverse scanning protocols according to our pilot study. Sn100kV, 90kV, and 120kV using flash mode at IQ20 are recommended for clinical applications considering both accuracy and radiation dose.

Keywords Photon-counting detector CT · Coronary artery calcification score · Agatston score · Radiation dose

Introduction

Coronary artery calcium (CAC) presents as a distinctive coronary artery disease manifestation, which is a potent predictor of cardiovascular morbidity and mortality [1–3]. The CAC quantification, accomplished through coronary artery calcium scores (CACS), including the Agatston, mass, and volume scores, holds significant clinical value and the

Agatston score is particularly vital for cardiovascular risk stratification and patient management [4–6].

Conventionally, standard CACS is derived from fixed scanning parameters, such as 2.5- or 3-mm slice thickness with 120 kV using sequence mode [7], which have remained largely unaltered amidst advances in CT technology, making it difficult to further reduce radiation exposure. While qualitative and quantitative assessments of CAC in non-gated CT have been explored to mitigate radiation dose, these approaches have not yet fully supplanted ECG-gated noncontrast cardiac CT in terms of accuracy [8]. The prospect of dose reduction through tube voltage reduction is promising, though the requisite standardization and implementation of corresponding threshold adjustments to get comparable CACS as standard CACS acquisition present challenges [9–11].

Recent studies in CT technology have ushered the era of photon-counting detector CT (PCD-CT) [12, 13]. In contrast to the conventional energy-integrating detector

---

Mengzhen Wang and Xu Zhang have contributed equally to this work and should be considered co-first authors.

✉ Wenjie Yang
   lisa_ywj@163.com

1   Department of Radiology, Ruijin Hospital, Shanghai Jiao Tong University School of Medicine, No.197 Ruijin Er Road, Shanghai 200025, China

2   Siemens Healthineers CT Collaboration, Shanghai, China

CT (EID-CT) involving the conversion of X-ray photons into visible light and then into an electrical signal − a process that can interfere with adjacent detector elements, the direct conversion of X-ray photons into an electrical signal in PCD-CT can avoid such interference [14]. Furthermore, unlike conventional CT using energy-integrating detectors that only acquire the total amount of energy across multiple photons concurrently, the photon-counting detector of PCD-CT can discriminate individual photon according to its energy from the X-ray beam, then making it possible to acquire high spatial resolution, less electronic noise, fewer beam-hardening artifacts and more stable Hounsfield unit (HU) numbers [15]. The potential to enhance quantitative CT applications lies in the consistency and standardization of CT values secondary to dual-source PCD-CT [16]. The accuracy and stability of CACS obtained through various scanning parameters, including the potential of reducing radiation dose and maintaining CACS stability on PCD-CT, remains unknown.

To test whether PCD-CT can result in accurate and stable CACS with different scanning protocols, we aimed to systematically evaluate CACS of PCD-CT using multiple tube voltages and scanning modes at different radiation dose levels in phantom and patients by using acquisitions on EID-CT as the reference.

Material and methods

Phantom study

In this study, a commercial static anthropomorphic chest phantom (QRM, Moehrendorf, Germany) was used (anterior posterior diameter, 20cm; lateral diameter, 30cm). The simulated coronary arteries (water-equivalent and CaHA material) contained six cylindrical inserts with different diameters (3 and 5 mm) and various densities (hydroxyapatite at 200, 400, and 800 mg/cm^3, indicating low, medium, and high density, respectively).

Phantom scan acquisition and reconstruction

For the reference acquisition, scanning was first performed on a conventional EID-CT (SOMATOM Force; Siemens Healthineers, Forchheim, Germany) using sequence mode with 120 kV to obtain the the gold standard CACS. Other detailed parameters are listed in Table 1. For PCD-CT (NAEOTOM Alpha; Siemens Healthineers GmbH) acquisition, 20 protocols using two scanning modes (sequence and "flash" [high-pitch spiral: pitch factor 3.2]) with five tube voltages (90 kV, 120 kV, 140 kV, 100 kV with tin filter [Sn100], and 140 kV with tin filter [Sn140]) and automatic tube current modulation (CARE Dose4D) at two image quality (IQ) levels optimized for non-contrast (low-IQ20; high-IQ42 or IQ50) were adapted. IQ 42 was used only for Sn100 because the highest IQ level of Sn100 is 42 and IQ 50 for the other tube voltage. Each of the scanning

Table 1 Scanning parameters of PCD-CT and EID-CT

Parameters	Phantom		Patient	
	EID-CT[#]	PCD-CT[##]	EID-CT[#]	PCD-CT[##]
Tube voltage [kV]	120	90, 120, 140, Sn100, Sn120, Sn140	120	120
Tube current [mAs]	38	7–141	40–85	11–22
ECG-pulsing window	/	/	65–85%	65–85%
IQ level	/	low (IQ20), high (IQ50 or 42)	/	IQ19
Scanning mode	Sequence	Sequence and flash	Sequence	Flash
Collimation [mm]	192*0.6	144*0.4	192*0.6	144*0.4
Rotation time [s/rot]	0.25	0.25	0.25	0.25
Field of view [mm]	220	220	220	220
Slice thickness/increment [mm]	3mm/1.5mm	3mm/1.5mm	3mm/1.5mm	3mm/1.5mm
Reconstruction kernel	QR36	QR36	QR36	QR36
Reconstruction algorithm	FBP	QIR 2	FBP	QIR 2
Matrix size [pixels]	512×512	512×512	512×512	512×512
Virtual monoenergetic level [keV]	/	70	/	70

[#]SOMATOM Force; Siemens Healthineers, Forchheim, Germany

[##]NAEOTOM Alpha; Siemens Healthineers GmbH

Sn- with tin filter

protocols was repeated three times. IQ level indicates the effective mAs that are applied for the reference water-equivalent diameter specific to the protocol along with a CT geometry correction, specifically for the focal spot to iso-center distance effect. As a result, the image quality level offers a definition of image quality that is independent of systems and reconstruction.

All acquisitions were then reconstructed via virtual monoenergetic imaging at 70 keV according to a previous study [17] with 3-mm slice thickness and 1.5-mm increments. The quantum iterative reconstruction (QIR) level was set at QIR2 by default setting.

All scanning parameters are listed in Table 1. For simplicity, we will denote the scan mode as "Scan mode, tube voltage_IQ level" next.

Patient study

Our study was approved by Ruijin Hospital Ethics Committee Shanghai Jiaotong University School of Medicine (Number 2023-186). All volunteers who were suspected of coronary artery disease (CAD) and indicated by clinicians for CCTA were recruited in September 2023, and all patients provided written informed consent. The inclusion criteria were as follows: (1) age > 18 years; and (2) previous chest CT or coronary CT angiography (CCTA) examination indicating coronary artery calcification.The exclusion criteria were as follows: (1) pregnant or lactating women; (2) coronary stents or coronary artery bypass graft surgery; (3) severe arrhythmia; and (4) chest CT or CCTA examination performed within a year (to avoid excessive radiation exposure). We recruite 15 patients but 12 patients were finally included after excluding two with severe atrial fibrillation and one with coronary stents.

Patient scan acquisition and reconstruction

All patients did not use any medical agents to control heart rate before CT examination. First, the EID-CT mentioned above in phantom scan was also used to scan the patients with sequence mode to obtain the referred ECG-gated CACS, followed by a PCD-CT ECG-gated CACS scanning on the same day. For PCD-CT scanning, the tube voltage was 120kV and current were determined using the automated tube current modulation (CARE Dose4D) with the IQ level set to 19. Then, the PCD-CT images were reconstructed at 70 keV according to the previous study[17]. The detailed scanning parameters are shown in Table 1. Volumetric Computed Tomography Dose Index (CTDIvol) and Dose-Length Product (DLP) were recorded from dose report automatically produced by CT system.

CACS measurement

Using a dedicated semi-automatic software (CT CaScoring, Syngo.Via, Version VB70; Siemens Healthineers), The CACS acquired from all scanning protocols was calculated on two separate occasions, with a 2-week interval between each calculation, by a radiologist with 3-year experience in cardiovascular imaging. The software identified all pixels with a density > 130 HU as calcification and the observer can correct the wrong segmentations manually. The factor used to calculate mass score was 0.743. For phantom, the Agatston, mass, and volume scores were calculated for each calcification (Fig. 1a). For the patients, the Agatston, mass, and volume scores were calculated at single lesion and patient level (Fig. 1b and 1c). CACS categories based on the Agatston score are as follows: 0, 1–10, 11–100, 101–400, and > 400 [7].

Figure 1a shows our phantom containing six hollow cylindrical hydroxyapatite calcifications of various sizes (large and small) and densities (200, 400, and 800 mg/cm^3). Figure 1b and 1c demonstrates the CACS of a 65-year-old male patient scanned using energy-integrating detector computed tomography (EID-CT) and photon-counting detector CT (PCD-CT), respectively.

Statistical analysis

In this study, two commercial statistical programs (SPSS, version 26 and R, version 4.1.3) were used. To test continuous data for normality, the Kolmogorov–Smirnov test was used. Data that conform to a normal distribution are expressed as mean ± standard deviation, whereas those with a non-normal distribution are reported as median (interquartile range). CACS and radiation dose differences between PCD-CT and EID-CT were compared using paired-samples t tests or Wilcoxon rank sum tests, depending on distribution. Agreements between PCD-CT- and EID-CT-derived CACS were assessed through intraclass correlation coefficient (ICC), Bland–Altman with 95% confidence interval limits of agreement (LoA), and root mean square error (RMSE) analysis. ICC was interpreted as follows: 0.0 to 0.3, lack of agreement; 0.31 to 0.5, weak agreement; 0.51 to 0.7, moderate agreement; 0.71 to 0.9, strong agreement; and 0.91 to 1.00, very strong agreement. Statistical significance was set at a P < 0.05.

Fig. 1 Coronary artery calcium score (CACS) measurement diagram of EID-CT and PCD-CT
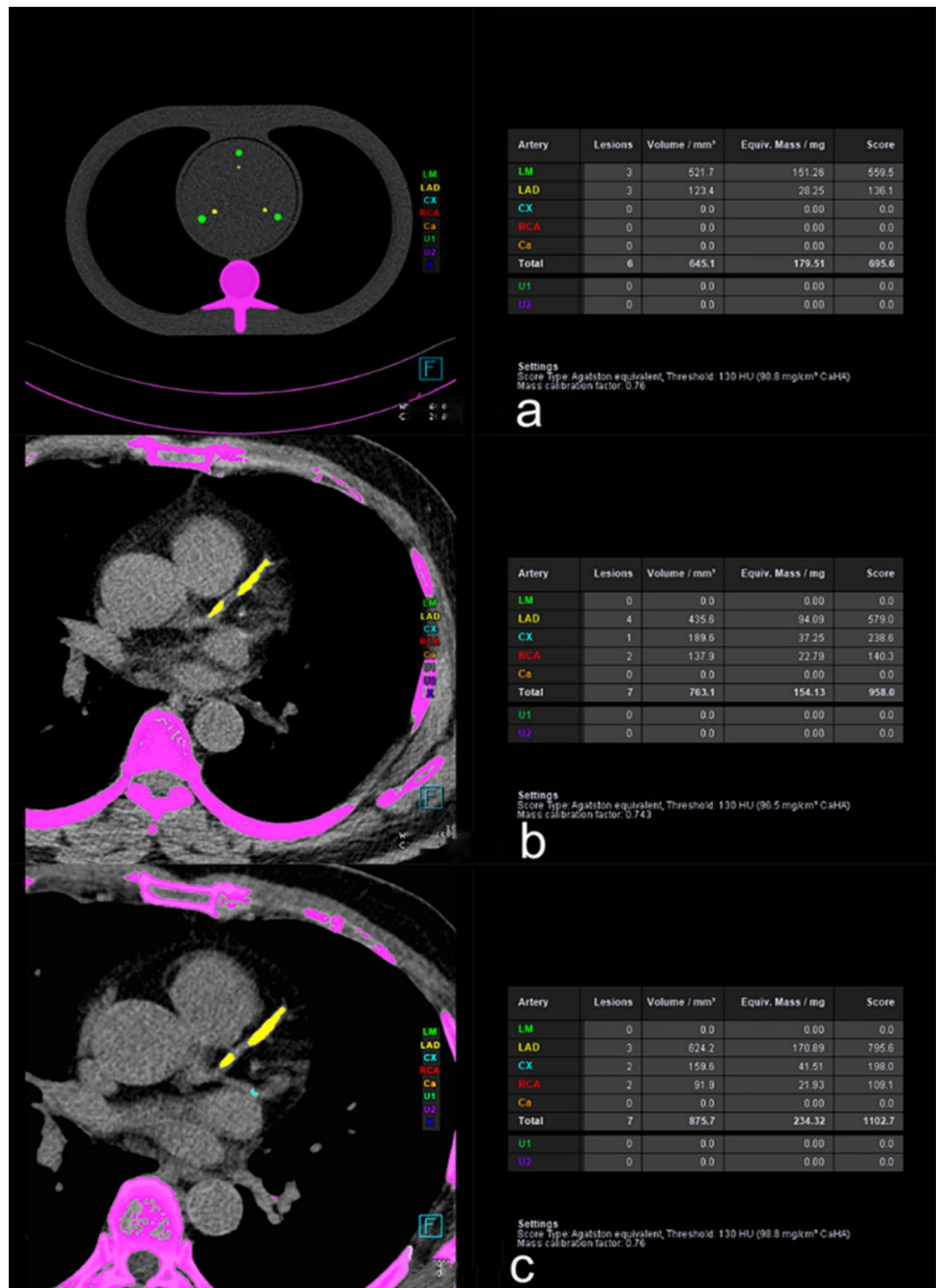
## Results

Radiation dose

In vitro

The CTDIvol of the phantom using the standard CACS scan protocol on EID-CT served as reference was 2.4 mGy and DLP was 31.1 mGy·cm, recorded form dose report provided by CT system, and SSDE was 4.2 mGy, calculated by the formula[18] CTDIvol, DLP and SSDE of all PCD-CT protocols were recorded in Supplementary materials-Table S1.

A radiation dose reduction (16–75%) from PCD-CT compared with the reference was obtained in all protocols using flash mode, with Flash spiral Sn100kV IQ20 got the lowest radiation dose (75% dose reduction). For sequence mode, only low IQ level (IQ20) got a radiation dose reduction (22–44%) while the high IQ level got a radiation dose increase(5–94%) compared with the reference, with Sn140 kV IQ50 got the highest radiation dose (94% increase) as shown in Fig. 2.

Fig. 2 Radiation dose reduction or increase of CACS scanning with PCD-CT compared with the reference
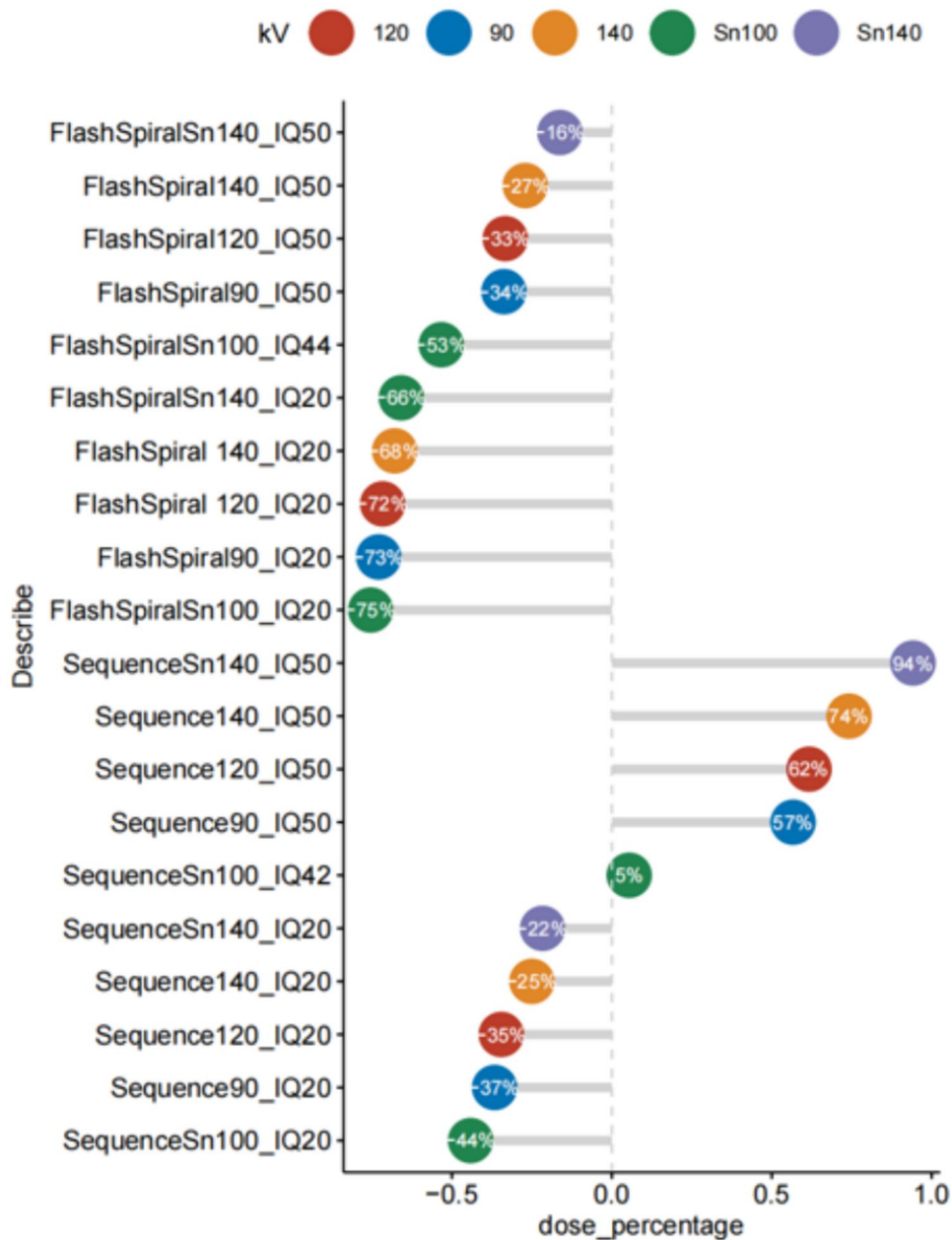
In vivo

A total of 12 patients (age, 69.83 ± 9.27 years, body mass index, 21.34 ± 1.72 kg/m²) with 28 calcified coronary arteries were finally recruited. The CTDIvol of the reference and PCD-CT were 2.21(1.94, 2.68) and 1.03(0.83, 1.51) mGy, respectively.

CACS analysis

In vitro

All intra-observer ICC of CACS were > 0.99. As shown in Table 2, there is no difference between Agatston and volume scores from all PCD-CT scans and the references (all

Table 2 Difference, intraclass correlation coefficient, and Bland–Altman analysis of CACS between PCD-CT and the references

Scanning mode/tube voltage(kV)/IQ level	Agatston score				Mass score				Volume score			
	Difference (p value)	ICC	Bias	LOA	Difference (p value)	ICC	Bias	LOA	Difference (p value)	ICC	Bias	LOA
Flash spiral /Sn100/IQ20	0.563	0.998[#]	1.535	− 11.201/11.201	0.000*	0.996[#]	− 1.674	− 5.012/1.664	0.966	0.998[#]	0.128	− 10.236/10.491
Flash spiral /Sn100/IQ44	1.000	0.998[#]	0.332	− 11.225/11.89	0.001*	0.997[#]	− 1.334	− 4.074/1.405	0.766	0.999[#]	0.267	− 4.856/5.390
Flash spiral /Sn140/Q20	0.563	0.998[#]	1.796	− 8.594/12.186	0.000*	0.996[#]	− 2.020	− 4.689/0.648	0.760	0.997[#]	0.298	− 11.922/12.518
Flash spiral/Sn140/IQ50	0.688	0.998[#]	− 0.637	− 11.554/10.281	0.001*	0.996[#]	− 1.740	− 5.148/1.667	0.663	0.999[#]	0.432	− 5.227/6.091
Flash spiral/120/IQ20	1.000	0.994[#]	− 1.704	− 22.591/19.182	0.000*	0.995[#]	− 1.831	− 5.812/2.150	0.098	0.999[#]	− 1.266	− 8.324/5.792
Flash spiral/140/IQ20	0.313	0.997[#]	3.086	− 10.145/16.316	0.008*	0.997[#]	− 1.348	− 4.846/2.150	0.181	0.999[#]	1.883	− 5.329/9.095
Flash spiral/120/IQ50	1.000	0.999[#]	0.400	− 6.927/7.727	0.000*	0.996[#]	− 1.899	− 4.841/1.043	0.000*	1.000[#]	− 1.353	− 3.349/0.644
Flash spiral/140/IQ50	0.563	0.997[#]	2.524	− 10.521/15.569	0.000*	0.997[#]	− 1.684	− 4.500/1.131	0.948	0.999[#]	0.105	− 6.395/6.605
Flash spiral/90/IQ20	0.563	0.995[#]	2.317	− 15.183/19.817	0.248	0.997[#]	− 0.851	− 4.861/3.158	0.671	0.997[#]	0.481	− 10.796/11.758
Flash spiral/90/IQ50	0.563	0.998[#]	− 1.382	− 13.502/10.738	0.000*	0.997[#]	− 1.492	− 4.049/1.065	0.008*	1.000[#]	− 1.344	− 4.935/2.246
Sequence/120/IQ20	1.000	0.997[#]	− 1.516	− 16.6/13.569	0.001*	0.996[#]	− 1.485	− 5.031/2.061	0.663	0.999[#]	− 0.411	− 6.719/5.898
Sequence/120/IQ50	0.219	0.997[#]	4.798	− 7.255/16.85	0.006*	0.999[#]	− 0.759	− 2.572/1.055	0.108	0.999[#]	1.507	− 5.004/8.018
Sequence/140/IQ20	0.438	0.997[#]	3.342	− 9.044/15.729	0.229	0.997[#]	− 0.696	− 4.328/2.936	0.000*	0.998[#]	4.202	− 1.541/9.946
Sequence/140/IQ50	0.313	0.996[#]	4.581	− 10.262/19.424	0.001*	0.999[#]	− 0.875	− 2.593/0.843	0.229	0.998[#]	2.107	− 6.148/10.361
Sequence/90/IQ20	0.094	0.997[#]	4.788	− 4.617/14.193	0.108	0.998[#]	− 0.444	− 3.991/3.103	0.061	0.997[#]	2.669	− 7.64/12.979
Sequence/90/IQ50	0.156	0.997[#]	4.950	− 5.423/15.323	0.151	1.000[#]	− 0.271	− 1.379/0.837	0.000*	0.999[#]	1.959	− 1.205/5.124
Sequence/Sn100/IQ20	0.438	0.996[#]	4.207	− 11.255/19.669	0.003*	0.999[#]	− 0.941	− 3.000/1.117	0.061	0.998[#]	1.442	− 6.952/9.836
Sequence/Sn100/IQ42	0.438	0.999[#]	1.288	− 5.072/7.649	0.000*	0.998[#]	− 1.243	− 3.569/1.083	0.640	1.000[#]	− 0.069	− 3.021/2.883
Sequence/Sn140/IQ20	0.563	0.997[#]	2.697	− 11.109/16.504	0.003*	0.998[#]	− 1.132	− 4.006/1.742	0.014*	0.999[#]	2.293	− 4.581/9.167
Sequence/Sn140/IQ50	0.563	0.998[#]	0.909	− 9.57/11.389	0.000*	0.997[#]	− 1.749	− 4.373/0.876	0.417	0.999[#]	− 0.773	− 7.317/5.771

Sn with tin filter, *IQ* image quality, *ICC* intraclass coefficient correlation, *LoA* limits of agreement

*P < 0.05

[#]P of ICC < 0.01

P > 0.05), except for the volume scores acquired from Flash Spiral 120 kV/90 kV_IQ50, as well as sequence 140 kV/Sn 140kV_IQ20 and sequence 90 kV_IQ50. However, mass scores were significantly higher (P < 0.05) for most PCD-CT settings than the references except Flash Spiral 90 kV_IQ20, sequence 90 kV_IQ20/50, and sequence 140 kV_IQ20 (all P > 0.05). ICC analysis showed strong agreements between Agatston, mass, and volume scores obtained with PCD-CT using various settings and references, with all ICC > 0.99 (Table 2).

Bland–Altman analysis (Table 2) revealed excellent agreements of CACS between PCD-CT and the reference. For Agatston score, the bias ranged from − 1.7 to 4.95, with only a single dot outside the LoA (Flash Spiral 90kV_IQ50) and Sequence Sn100kV_IQ42 obtained the narrowest LoA (12.72). For the mass scores, the bias spanned from − 2.02 to − 0.27, with only three dots outside the LoA (Flash Spiral Sn140kV_IQ20) and Sequence 90kV_IQ50 obtained the narrowest LoA (1.33). For the volume score the bias extended from − 1.35 to 4.20, with only one dot outside the LoA (Flash Spiral 120kV_IQ50 and Sequence 140kV_IQ20) and Sequence 90kV_IQ50 obtained the narrowest LoA (3.73).

For all PCD-CT scannnig modes, Fig.S1 illustrates that the RMSE of the Agatston score between PCD-CT and the reference ranged from 5 to 11.5. For the 200, 400, and 800 mg/cm^3 calcification, RMSE (Fig.S2-4) ranged from 1.4 to 10.9, 6.8–18.3, and 1.8–10.9, respectively. Bland–Altman and ICC analysis also showed high Agatston score agreements between all PCD-CT scanning settings and the reference, with all dots in the LoA (bias range, 0.6/10.1, − 14.8/ − 0.4, − 10.8/0.2, respectively) and all ICC > 0.90.

The Agatston score of calcifications with different sizes and densities scanned with PCD-CT using various scanning modes presented good agreements with the references (Fig. 3), except for the calcification with both low density and small size (200 mg/cm^3, 3mm).

In-vivo

All intra-observer ICC of CACS at the single calcified plaque level was > 0.99. Agatston, volume, and mass scores of the patients were 494.45(142,45, 1187.05), 417.45(136.25, 1046), and 114.46(23.87, 250.13) for the EID-CT and 514.9(175.33, 1302.6), 454.95(156.98, 1111.63), and 123.58(29.91, 286.03) for the PCD-CT, respectively. The radiation dose of PCD-CT was significantly lower than that of EID-CT (CTDIvol, 1.03[0.83, 1.51] vs. 2.21[1.94, 2.68]mGy, p < 0.001). Table 3 shows the CACS of EID-CT and PCD-CT. At both the single lesion and patient levels, Bland–Altman analysis (Fig. 4) and ICC (from 0.991 to 0.998) showed good agreements between the PCD-CT and

EID-CT. No significant difference was found for the CACS categories (P = 0.317), except for one patient who upgraded from 100 to 400 to > 400.

Discussion

In our in vivo and in vitro study, we comprehensively evaluated the accuracy of CACS with various scan settings acquired from PCD-CT. In the in vitro settings, we ascertained that the CACS measurements acquired from PCD-CT, spanning varying tube voltages, scanning modes, and IQ levels reconstructed at 70 keV, remain accurate and reproducible and the results were also validated in patients.

CACS has been widely used routinely in clinics to quantify coronary calcification. Precise and reproducible CACS measurement is imperative for guiding clinical patient management [4–6]. However, CACS is susceptible to scan parameters, particularly varying tube voltages [19–21], which may compromise CACS reproducibility and affect the monitoring of coronary artery sclerosis progress. The standard scanning tube voltage for CACS is 120 kV [7], which is insufficient to satisfy the requirement of radiation exposure reduction. No widely acknowledged thresholds complementary to the low tube voltages exist currently, although many studies have put forward different adjusted thresholds for varying tube voltages and reconstruction algorithms [22–24].

Since the combination of dual-source and PCD techniques enables spectral imaging with high temporal resolution and spatial resolution [25], which may provide high CT value accuracy at low-dose levels, and the consistency and standardization of CT values provided by PCD-CT improved the screening and monitoring of calcium plaques. This property has been validated by several phantom studies [26, 27] and holds great potential in advancing quantitative application of CT such as CACS. Confirming whether the parameter measurements of PCD-CT now extensively employed in clinical practice such as CACS are accurate is therefore requisite.

A previous study found that CACS reconstructed with 70 keV obtained from various voltages (70kV, 90kV, Sn100kV, Sn140kV, and 140 kV) at the same IQ levels yielded comparable results to a 120 kV reference [28]. However, there is no systematic analysis was not conducted for CACS obtained from PCD-CT with different tube current and scanning modes. Furthermore, the agreement and variability of CACS between conventional EID-CT and PCD-CT were absent, and the established risk catergories of CACS was based on EID-CT, making it necessary to validate the comparability of CACS between PCD-CT and EID-CT. Similarly, several previous phantom studies explored the accuracy of PCD-CT CACS
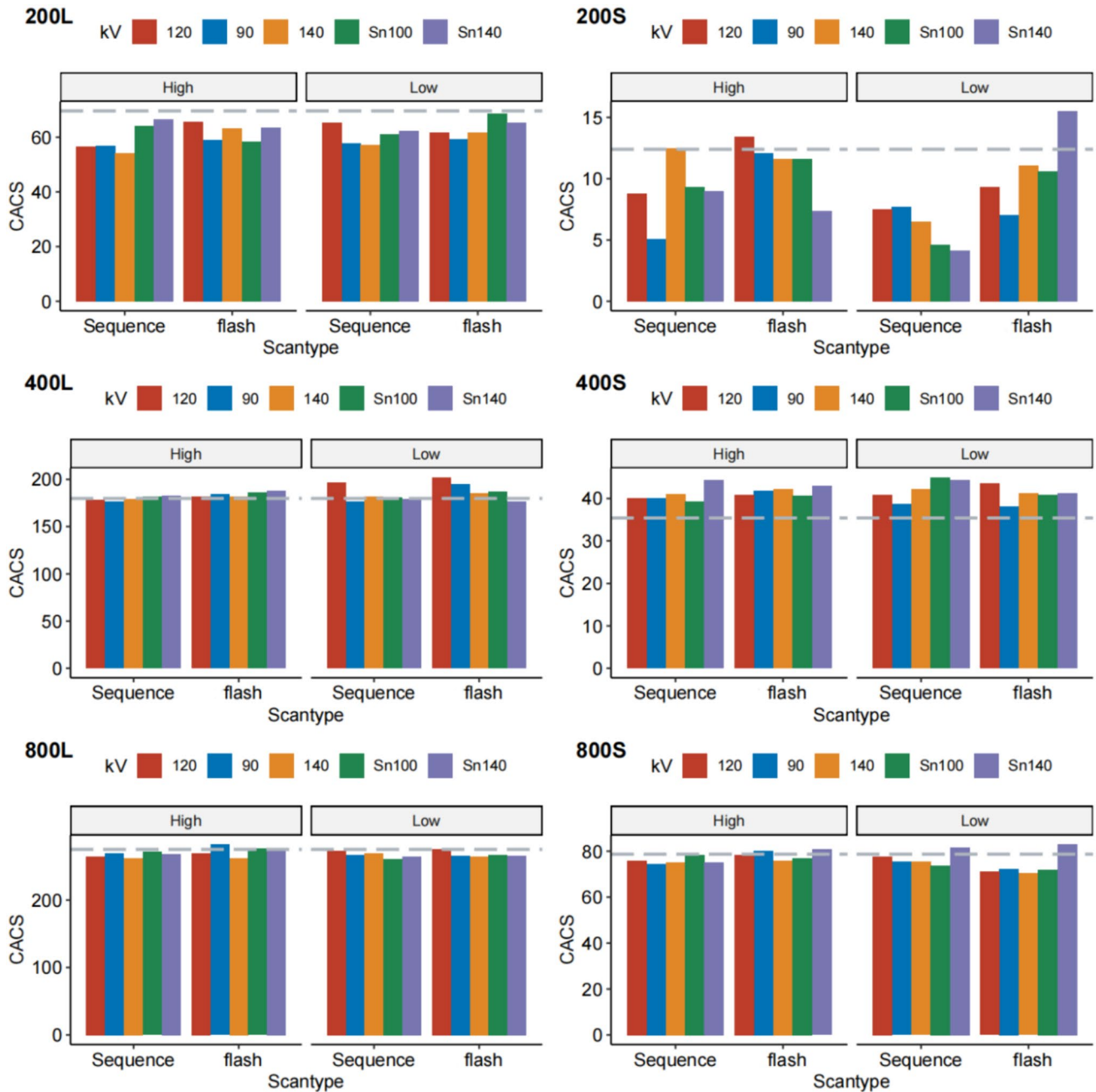
Fig. 3 Bar chart of the Agatston score of phantom with different sizes and densities scanned on PCD-CT with different radiation doses. L and S indicate large and small sizes with 5 and 3mm diameter, respectively. 200, 400, and 600 indicate different densities (200, 400, and 600 mg/cm³). Low and high indicate a low radiation dose (IQ level at 20) and high radiation dose (IQ level at 42 or 50), respectively. Flash indicates flash spiral mode (high pitch 3.2). The grey dashed line indicates the CACS of EID-CT

at different tube voltages; however, none of these studies validated their findings in patients [28–30]. Although Eberhard *M's* study encompassed both the phantom and patients, but they only analyzed the accuracy of PCD-CT CACS acquired using 120 kV in the phantom [31]. Our study presents a comprehensive exploration of the accuracy of CACS using different scan modes and tube voltages at different radiation dose levels in the phantom, as

well as a validation of these findings in a small cohort of patients by using 120 kV sequence scanning on EID-CT as reference.

In our study, we assessed not only Agatston scores but also mass and volume scores by using simulating calcification with different densities in detail. Our findings were inconsistent with the study by van der Werf NR [30], which demonstrated clinically relevant differences from the

Table 3 Radiation dose and CACS of PCD-CT and EID-CT in patients

	EID-CT	PCD-CT	P value
Heart rate [beats/min]	71.5(64.5, 85.75)	69.5(62, 84.5)	0.342
CTDIvol [mGy]	2.21(1.94, 2.68)	1.03(0.83, 1.51)	0.004
DLP [mGy·cm]	33.95(27.68, 40.55)	20.5(16.5, 26.98)	0.002
Single calcified plaque level			
Volume score	58.9 (25.8, 167.1)	62.5 (27.3, 171.0)	0.002
Mass score	11.3 (4.0, 36.3)	13.3 (4.9, 42.5)	<0.001
Agatston score	74.8 (22.5, 203.8)	81.5 (26.7, 193.5)	0.002
Patient level			
Volume score	417.5(136.3, 1046.0)	455.0(157.0, 1111.6)	0.002
Mass score	114.5(23.9, 250.1)	123.6(29.9, 286.0)	0.002
Agatston score	494.5(142.5, 1187.1)	514.9(175.3, 1302.6)	0.005

CTDIvol volumetric computed tomography dose index, *DLP* dose-length product
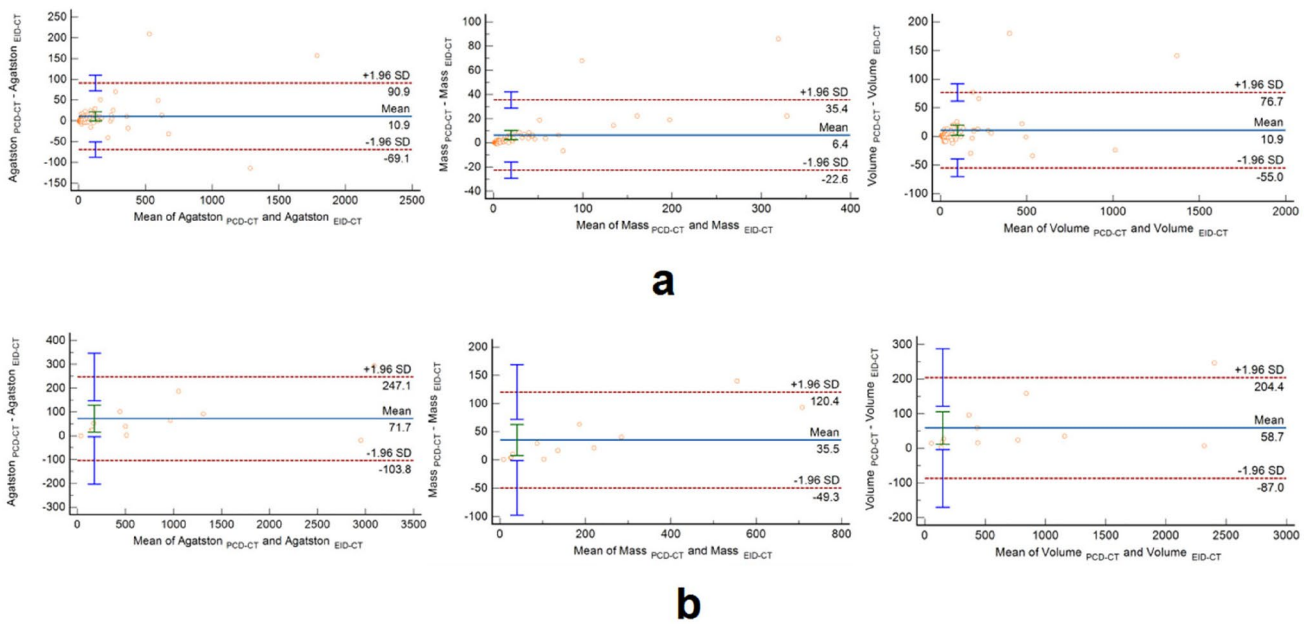
Fig. 4 Bland–Altman analysis of CACS in vivo between PCD-CT and the reference. **a** shows CACS at the single lesion level and **b** shows CACS at the patient level

reference in low-density calcification when using reduced tube current protocols, whereas our study demonstrates that PCD-CT achieves a minor Agatston score RMSE relative to the reference for low-density calcification. However, our study found that the mass scores derived from PCD-CT demonstrated a relatively greater deviation from references than the Agatston and volume scores. The mass score is calculated as the product of the calibration factor, volume, and mean attenuation values for each calcification [8], whereas the traditional CACS is calibrated and converted using 120 kV tube voltage. In the context of our study, the decision to employ 70 keV images was based on that 70 keV images are the most similar to 120 kV images among the mono-energetic images, which was also adapted by a prior Agatston score phantom study [17]. The calibration factor and this specific choice of energy level may need further be elaborated for accurate mass score calculation on PCD-CT.

This study has the following limitations: (1) Our phantom classifications were stationary and homogeneous; however, we subsequently performed patient validation, which to some extent compensated for this limitation. (2) The number of included patients was small, which might reduce the statistical power to assess whether PCD-CT led to CACS reclassification. Moreover, the sample size needs to be expanded in the future. (3) The effect of different QIR and keV levels of PCD-CT on CACS was not explored because

our study purpose was to explore the effect of scanning parameters and not reconstruction parameters on CACS, the latter of which has been investigated in previous studies.

Conclusions

In conclusion, PCD-CT employing different tube voltages, scanning modes, and IQ levels can generate an accurate and repeatable CACS, improving atherosclerotic disease screening and monitoring. Sn100kV, 90kV, and 120kV using flash mode at IQ20 are recommended for clinical applications considering both accuracy and radiation dose.

Supplementary Information The online version contains supplementary material available at https://doi.org/10.1007/s10554-024-03209-5.

Data availability No datasets were generated or analysed during the current study.

Declarations

Competing interests Zhihan Xu is an employee of Siemens Healthineers. The remaining authors declare that they have no conflict of interest with each other.

References

1. Shemesh J, Henschke CI, Shaham D et al (2010) Ordinal scoring of coronary artery calcifications on low-dose CT scans of the chest is predictive of death from cardiovascular disease. Radiology 257(2):541–548. https://doi.org/10.1148/radiol.10100383
2. Lei MH, Wu YL, Chung SL et al (2021) Coronary artery calcium score predicts long-term cardiovascular outcomes in asymptomatic patients with type 2 diabetes. J Atheroscler Thromb 28(10):1052–1062. https://doi.org/10.5551/jat.59386
3. Church TS, Levine BD, McGuire DK et al (2007) Coronary artery calcium score, risk factors, and incident coronary heart disease events. Atherosclerosis 190(1):224–231. https://doi.org/10.1016/j.atherosclerosis.2006.02.005
4. Patel J, Pallazola VA, Dudum R et al (2021) Assessment of coronary artery calcium scoring to guide statin therapy allocation according to risk-enhancing factors: the multi-ethnic study of atherosclerosis. JAMA Cardiol 6(10):1161–1170. https://doi.org/10.1001/jamacardio.2021.2321
5. Ferket BS, Hunink MGM, Masharani U et al (2022) Lifetime cardiovascular disease risk by coronary artery calcium score in individuals with and without diabetes: an analysis from the multi-ethnic study of atherosclerosis. Diabetes Care 45(4):975–982. https://doi.org/10.2337/dc21-1607
6. Parcha V, Malla G, Kalra R et al (2021) Coronary artery calcium score for personalization of antihypertensive therapy: a pooled cohort analysis. Hypertension 77(4):1106–1118. https://doi.org/10.1161/HYPERTENSIONAHA.120.16689
7. Leipsic J, Abbara S, Achenbach S et al (2014) SCCT guidelines for the interpretation and reporting of coronary CT angiography: a report of the society of cardiovascular computed tomography guidelines committee. J Cardiovasc Comput Tomogr 8(5):342–358. https://doi.org/10.1016/j.jcct.2014.07.003
8. Alluri K, Joshi PH, Henry TS et al (2015) Scoring of coronary artery calcium scans: history, assumptions, current limitations, and future directions. Atherosclerosis 239(1):109–117. https://doi.org/10.1016/j.atherosclerosis.2014.12.040
9. Grani C, Vontobel J, Benz DC et al (2018) Ultra-low-dose coronary artery calcium scoring using novel scoring thresholds for low tube voltage protocols-a pilot study. Eur Heart J Cardiovasc Imaging 19(12):1362–1371. https://doi.org/10.1093/ehjci/jey019
10. Nakazato R, Dey D, Gutstein A et al (2009) Coronary artery calcium scoring using a reduced tube voltage and radiation dose protocol with dual-source computed tomography. J Cardiovasc Comput Tomogr 3(6):394–400. https://doi.org/10.1016/j.jcct.2009.10.002
11. Kim S, Lee CJ, Han K et al (2021) Histogram-derived modified thresholds for coronary artery calcium scoring with lower tube voltage. Sci Rep 11(1):17450. https://doi.org/10.1038/s41598-021-96695-9
12. Rajendran K, Petersilka M, Henning A et al (2022) first clinical photon-counting detector CT system: technical evaluation. Radiology 303(1):130–138. https://doi.org/10.1148/radiol.212579
13. Si-Mohamed SA, Boccalini S, Lacombe H et al (2022) Coronary CT angiography with photon-counting CT: first-in-human results. Radiology 303(2):303–313. https://doi.org/10.1148/radiol.211780
14. Flohr T, Petersilka M, Henning A et al (2020) Photon-counting CT review. Phys Med 79:126–136. https://doi.org/10.1016/j.ejmp.2020.10.030
15. Willemink MJ, Persson M, Pourmorteza A et al (2018) Photon-counting CT: technical principles and clinical prospects. Radiology 289(2):293–312. https://doi.org/10.1148/radiol.2018172656
16. McCollough CH, Rajendran K, Leng S (2023) Standardization and quantitative imaging with photon-counting detector CT. Invest Radiol 58(7):451–458. https://doi.org/10.1097/RLI.0000000000000948
17. van der Werf NR, Greuter MJW, Booij R et al (2022) Coronary calcium scores on dual-source photon-counting computed tomography: an adapted Agatston methodology aimed at radiation dose reduction. Eur Radiol 32(8):5201–5209. https://doi.org/10.1007/s00330-022-08642-5
18. Boone JM, Strauss KJ, Cody DD et al (2011) Report No. 204 - Size-specific dose estimate in pediatric and adult body CT examinations. American Association of Physicists in Medicine. https://doi.org/10.37206/143
19. Zhang D, Scott A, Lee C et al (2021) Coronary artery calcium scoring at lower tube voltages—dose determination and scoring mechanism. Eur J Radiol 139:109680. https://doi.org/10.1016/j.ejrad.2021.109680
20. Allio IR, Caobelli F, Popescu CE et al (2022) Low-dose coronary artery calcium scoring compared to the standard protocol. J Nucl Cardiol. https://doi.org/10.1007/s12350-022-03120-3
21. Fujioka C, Funama Y, Kiguchi M et al (2012) Coronary artery calcium scoring on different 64-detector scanners using a low-tube voltage (80 kVp). Acad Radiol 19(11):1402–1407. https://doi.org/10.1016/j.acra.2012.07.003
22. Marwan M, Mettin C, Pflederer T et al (2013) Very low-dose coronary artery calcium scanning with high-pitch spiral acquisition

mode: comparison between 120-kV and 100-kV tube voltage protocols. J Cardiovasc Comput Tomogr 7(1):32–38. https://doi.org/10.1016/j.jcct.2012.11.004

23. Thomas CK, Muhlenbruch G, Wildberger JE et al (2006) Coronary artery calcium scoring with multislice computed tomography: in vitro assessment of a low tube voltage protocol. Invest Radiol 41(9):668–673. https://doi.org/10.1097/01.rli.0000233324.09603.dd

24. Kamani CH, Huang W, Lutz J et al (2022) Impact of adaptive statistical iterative reconstruction-v on coronary artery calcium scores obtained from low-tube-voltage computed tomography—a patient study. Acad Radiol 29(Suppl 4):S11–S16. https://doi.org/10.1016/j.acra.2020.10.025

25. Euler A, Higashigaito K, Mergen V et al (2022) High-pitch photon-counting detector computed tomography angiography of the aorta: intraindividual comparison to energy-integrating detector computed tomography at equal radiation dose. Invest Radiol 57(2):115–121. https://doi.org/10.1097/RLI.0000000000000816

26. Liu LP, Shapira N, Chen AA et al (2022) First-generation clinical dual-source photon-counting CT: ultra-low-dose quantitative spectral imaging. Eur Radiol 32(12):8579–8587. https://doi.org/10.1007/s00330-022-08933-x

27. Symons R, Reich DS, Bagheri M et al (2018) Photon-counting computed tomography for vascular imaging of the head and neck: first in vivo human results. Invest Radiol 53(3):135–142. https://doi.org/10.1097/RLI.0000000000000418

28. Dobrolinska MM, van der Werf NR, van der Bie J et al (2023) Radiation dose optimization for photon-counting CT coronary artery calcium scoring for different patient sizes: a dynamic phantom study. Eur Radiol. https://doi.org/10.1007/s00330-023-09434-1

29. Mergen V, Higashigaito K, Allmendinger T et al (2021) Tube voltage-independent coronary calcium scoring on a first-generation dual-source photon-counting CT-a proof-of-principle phantom study. Int J Cardiovasc Imaging. https://doi.org/10.1007/s10554-021-02466-y

30. van der Werf NR, van Gent M, Booij R et al (2021) Dose reduction in coronary artery calcium scoring using mono-energetic images from reduced tube voltage dual-source photon-counting CT data: a dynamic phantom study. Diagnostics (Basel). https://doi.org/10.3390/diagnostics11122192

31. Eberhard M, Mergen V, Higashigaito K et al (2021) Coronary calcium scoring with first generation dual-source photon-counting CT-first evidence from phantom and in-vivo scans. Diagnostics (Basel). https://doi.org/10.3390/diagnostics11091708